3D modelling of rock mass falls using the Particle Flow Code PFC^{3D}

A. Preh & R. Poisel
Institute for Engineering Geology, Vienna University of Technology, Vienna, Austria

ABSTRACT: Rock mass falls are modelled as the movements of single rock blocks over a surface or as the movement of a viscous mass over a surface (DAN). In reality a mass of discrete, interacting rock blocks is moving downslope. Thus, the program PFC (Particle Flow Code) based on the Distinct Element Method was used to model rock mass falls realistically in 3 dimensions, based on physical relations. PFC models the movement and interaction of circular (2D) or spherical (3D) particles and wall elements, using the laws of motion and of force - displacement. During the calculation, the contacts between particles and particles or particles and walls are detected automatically. The particles may be bonded together at their contact points, and the bondage can break due to an impact. For realistic modelling of a runout a viscous damping routine in case of a particle – wall contact was introduced. Numerical drop tests, comparisons with the results of a rock fall program and back analyses of several rock mass falls provided appropriate damping factors. Thus, the movement types - bouncing, sliding, rolling and free falling of single rock blocks - and the interaction between the blocks occurring in a rock mass fall can be realistically modelled by using the PFC adapted code.

1 METHODS TO MODEL A ROCK MASS FALL USING PFC

PFC models the movements and interactions of stressed assemblies of spherical particles either in or getting into contact with wall elements. The particles may be bonded together at their contact points to represent a solid that may fracture due to progressive bond breakage.

Every particle is checked on contact with every other particle at every time step. Thus, PFC can simulate not only failure mechanisms of rock slopes but also the runout of a detached and fractured rock mass (Poisel & Roth 2004).

Rock mass falls can be modelled as an "All Ball model" and a "Ball Wall model". An "All Ball model" (Fig. 1) simulates the slope as an assembly of balls bonded together. The simulation shows the failure mechanism of the slope due to gravity (Poisel & Preh 2004). After detachment of the moving mass, the runout is modelled automatically. As in every other numerical model, the material represents only a hypothetical material. In reality, a large number of blocks are moving downslope. Due to a restricted number of balls, due to software and computation time reasons, it is generally not possible to model every rock block with a single ball.

In the "Ball Wall model" (Fig. 2) the underlying bedrock is simulated by linear (2D) and planar (3D) wall elements (Roth 2003). Therefore, an estimate or a model of the failure mechanism of the slope and of the detachment mechanism is needed as an input parameter. However, in the "Ball Wall model" the detached mass can be modelled using more and smaller balls with the same computational effort in order to approach reality better. The "Ball Wall model" offers the possibility to make use of the know-how related to runout relevant factors (coefficients of restitution, absorption, friction, etc.) applied in rock fall programs (Hoek 1987, Spang & Rautenstrauch 1988).

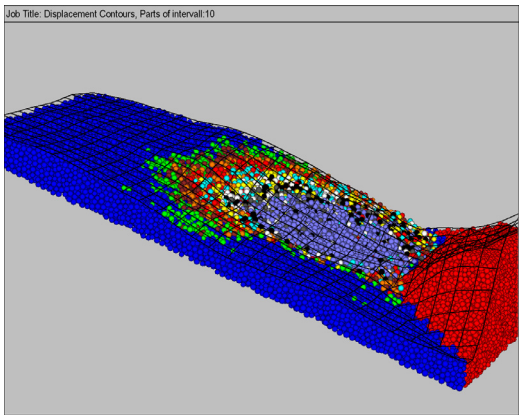

Figure 1. All Ball model (Preh 2004)

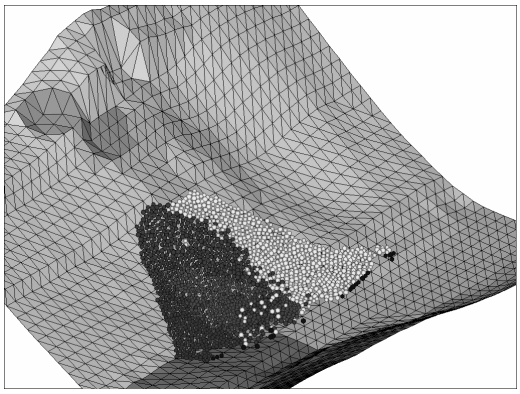

Figure 2. Ball Wall model (Frühwirth 2004)

2 RUNOUT RELEVANT PARAMETERS

According to observations in nature, several kinds of movements of the rock fall process (Broilli, 1974) have to be distinguished during the computation (Bozzolo, 1987):

- free falling,
- bouncing,
- rolling and
- sliding.

In order to achieve an appropriate simulation of these different kinds of movements by PFC, some modifications have been necessary using the implemented programming language (Fish).

2.1 *Free falling*

In order to model the free falling of blocks, neither the acceleration nor the velocity (ignoring the air resistance) is to be reduced during fall as a consequence of mechanical damping.

PFC applies a local, non- viscous damping proportional to acceleration, to the movement of every single particle as a default. The local damping used in PFC is similar to that described in Cundall (1987). A damping-force term is added to the equations of motion, so that the damped equations of motion can be written

$$F_{(i)} + F^{d}_{(i)} = M_{(i)}A_{(i)}; \quad i = 1\ldots6 \tag{1}$$

$$M_{(i)}A_{(i)} = \begin{cases} m\ddot{x}_{(i)} & \text{for } i = 1\ldots3; \\ I\dot{\omega}_{(i-3)} & \text{for } i = 4\ldots6 \end{cases} \tag{2}$$

where $F_{(i)}$, $M_{(i)}$, and $A_{(i)}$ are the generalized force, mass, and acceleration components, I is the principal moment of inertia, $\dot{\omega}$ is the angular acceleration and $\ddot{x}$ is the translational acceleration; $F_{(i)}$ includes the contribution from the gravity force; and $F^{d}_{(i)}$ is the damping force

$$F^{d}_{(i)} = -\alpha\left|F_{(i)}\right|\text{sign}(v_{(i)}) \quad i = 1\ldots6 \tag{3}$$

expressed in terms of the generalized velocity

$$v_{(i)} = \begin{cases} \dot{x}_{(i)} & \text{for } i = 1\ldots3; \\ \omega_{(i-3)} & \text{for } i = 4\ldots6. \end{cases} \tag{4}$$

The damping force is controlled by the damping constant α, whose default value is 0.7 and which can be separately specified for each particle.

This damping model is the best suited for a quick calculation of equilibrium. There arises, however, the disadvantage of the movements of the particles being damped as well. Therefore, the local damping has been deactivated for all kinds of particle movements.

2.2 *Bouncing*

Elastic and plastic deformations occur in the contact zone during the impact of a block. Both the kinetic energy of the bouncing block and the rebound height are reduced by the deformation work. The reduction of the velocity caused by the impact is modelled with the help of a viscous damping model integrated in PFC.

The viscous damping model used in PFC introduces normal and shear dashpots at each contact (Fig. 3). A damping force, D_i (i = n: normal, s: shear), is added to the contact force, of which the normal and shear components are given by

$$D_i = C_i \cdot \left|V_i\right| \tag{5}$$

where C_i (i = n: normal, s: shear) is the damping constant, V_i (i = n: normal, s: shear) is the relative velocity at contact, and the damping force acts to oppose motion. The damping constant is not specified directly; instead, the critical damping ratio β_i (i = n: normal, s: shear) is specified, and the damping constant satisfies

$$C_i = \beta_i \cdot C_i^{crit} \tag{6}$$

where C^{crit}_i is the critical damping constant, which is given by

$$C_i^{crit} = 2m\omega_i = 2\sqrt{mk_i} \tag{7}$$

where ω_i (i = n: normal, s: shear) is the natural frequency of the undamped system, k_i (i = n: normal, s: shear) is the contact tangent stiffness, and m is the effective system mass.

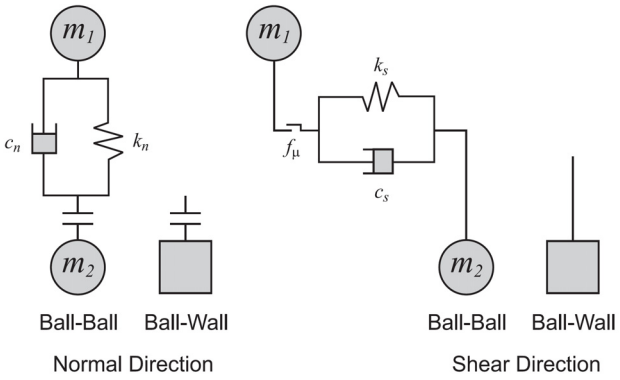

Figure 3. Viscous damping activated at a contact with the linear contact model (Itasca 1999)

In rock fall programs, the rebound height of blocks touching the bedrock is calculated using restitution coefficients. The restitution coefficient R_i (i = n: normal, s: shear) is defined as the ratio of the contact velocity before and after the impact and can be defined as

$$R_i = \frac{v_i^f}{v_i^i} \tag{8}$$

where v_i^f (i = n: normal, s: shear) is the velocity of the block after impact and v_i^i (i = n: normal, s: shear) is the velocity of the object before impact. The relation between the restitution coefficient R_i and the critical damping ratio β_i can be estimated by simulating drop tests (Fig. 4).

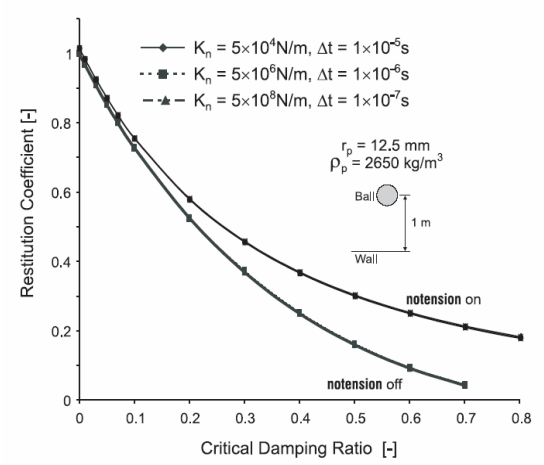

Figure 4. Relation between restitution coefficient and critical damping ratio (Itasca 1999)

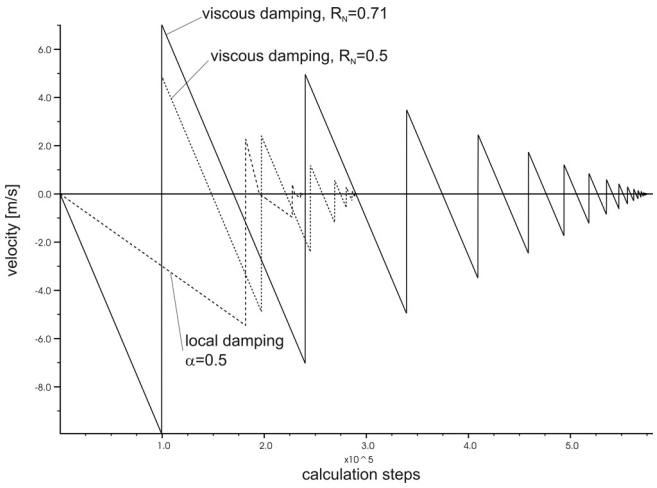

Figure 5. Drop tests, course of velocity: dashed line – local damping $\alpha = 0.7$, full line – $R_N = 0.71$, dotted line – $R_N = 0.5$

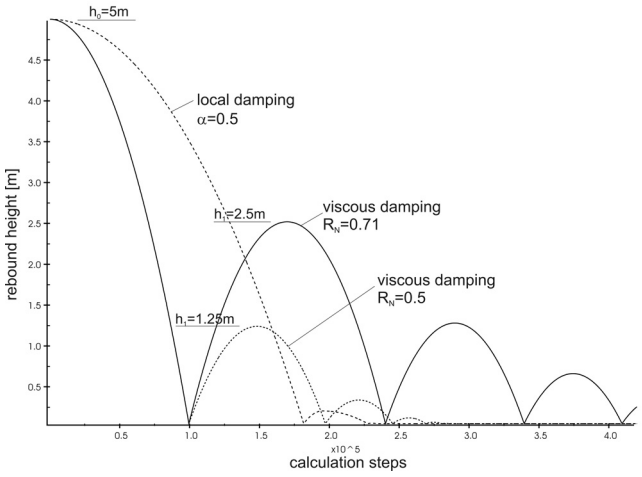

Figure 6. Drop tests, rebound height: dashed line – local damping $\alpha = 0.7$, full line – $R_N = 0.8$, dotted line – $R_N = 0.5$

Figures 5 and 6 show the results of a drop test for verification of the viscous damping model, where the rebounds of three differently damped particles have been investigated: the first one using the default value of the non viscous damping ($\alpha = 0.7$), the second one using the viscous damping with a critical damping ratio β_n of 0.27 and the third one using the viscous damping with a critical damping ratio β_n of 0.12.

The critical damping ratios selected for this comparison equal the restitution coefficient $R_N = 0.5$ ($\beta_n = 0.27$) and 0.71 ($\beta_n = 0.12$) according to the drop tests back calculated by Itasca (Fig. 4) This is verified by the course of the particle velocities (Fig. 5).

According to the conservation of energy, a restitution coefficient $R_N = 0.5$ results in a rebound height of a quarter of the drop height and a restitution coefficient $R_N = 0.71$ results in a rebound height of half the drop height. This is verified by the course of the rebound height (Fig. 6).

Thus, it is possible to control the number of impacts as well as the magnitude of the bouncing height, using the viscous contact damping model.

Spin has an impact on both the direction and the velocity of the rebounding block. Therefore, it is essential to consider the spinning when modelling the runouts of rock falls. PFC determines the motion of a each single particle by the resultant force and moment vectors acting upon it, and describes it in terms of the translational motion of a point in the particle and the rotational motion of the particle (Equations 1 and 2). Figure 7 depicts the flight trajectories of three particles bouncing at different spins.

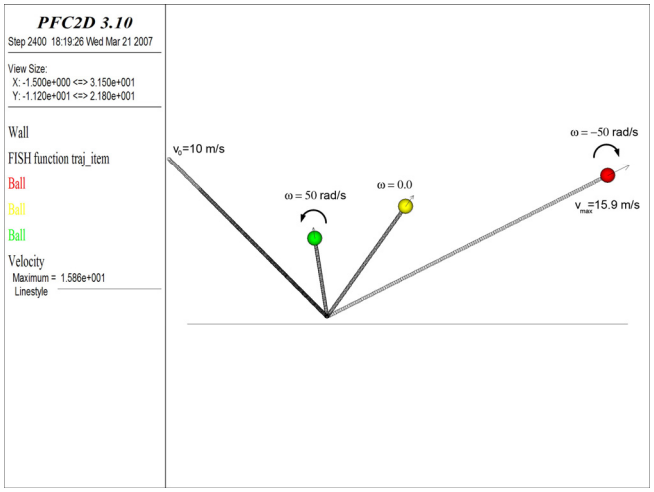

Figure 7. Rebound angle influenced by the particle spin (black line – rebound course; green, yellow and red balls – particle position after rebound)

Furthermore, with PFC the interaction of friction and spin is considered, since the influence of the spin increases with the increase of frictional resistance.

By modelling rock mass falls, it was shown to be necessary to distinguish between ball-ball contacts and ball-wall contacts. This was done by using the programming language Fish.

2.3 *Rolling*

The most important runout relevant effect is rolling resistance, because it is known that pure rolling of blocks in

the model leads to more extensive runouts than observed in nature.

The rolling resistance is caused by the deformation of the rolling body and/or the deformation of the ground (Fig. 8) and depends strongly on the ground and the block material.

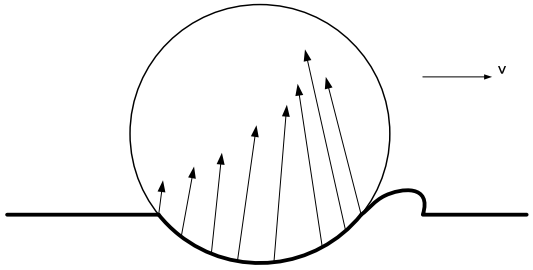

Figure 8. Deformation of the surface and distribution of contact stresses

Due to these deformations, the distribution of contact stresses between the ground and the block is asymmetric (Fig. 9). Replacing the contact stresses by equivalent static contact forces results in a normal force N, which is shifted forward by the distance of c_{rr} , and a friction force F_{rr} , opposing the direction of the movement.

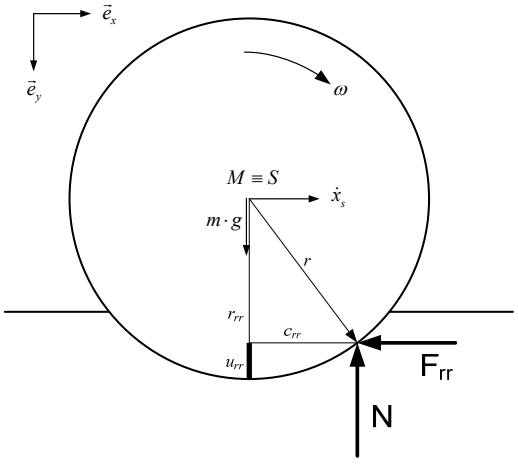

Figure 9. Calculation of the rolling resistance

The deceleration of the angular velocity caused by the rolling resistance is calculated using conservation of translational momentum (Equation 9) and angular momentum (Equation 10).

$$m \cdot \ddot{x}_s = -F_{rr} \tag{9}$$

$$-I \cdot \dot{\omega}_{rr} = M_{rr}, \; I_{sphere} = \frac{2}{5} \cdot m \cdot r^2 \tag{10}$$

where M_{rr} is the resulting moment caused by the rolling resistance, I is the principal moment of inertia and ω_{rr} is the angular deceleration.

The kinematic link is established by the condition of pure rolling (Equation 11).

$$\ddot{x}_s = \dot{\omega} \cdot r \tag{11}$$

The angular acceleration is defined by a finite difference relation in order to express the increment of the angular velocity per time increment (Equation 12). Thus, the friction force $F_{rr\,i}$ is defined by the conservation of momentum

$$F_{rr} = -m \cdot \frac{\Delta\omega_{rr}}{\Delta t} \cdot r \cdot \tag{12}$$

Equation 10 and equation 12 yield

$$-\frac{2}{5} \cdot m \cdot r^2 \cdot \frac{\Delta\omega_{rr}}{\Delta t} = F_{rr} \cdot r_{rr} - N \cdot c_{rr} \tag{13}$$

$$-\frac{2}{5} \cdot m \cdot r^2 \cdot \frac{\Delta\omega_{rr}}{\Delta t} = -m \cdot \frac{\Delta\omega_{rr}}{\Delta t} \cdot r \cdot r_{rr} - m \cdot g \cdot c_{rr} \cdot$$

Therefore, the angular deceleration is

$$\Delta\omega_{rr} = \frac{-g \cdot c_{rr}}{r \cdot (r_{rr} - \frac{2}{5} \cdot r)} \cdot \Delta t \tag{14}$$

$$r_{rr} = \sqrt{r^2 - c_{rr}^2} \cdot$$

The rolling resistance is implemented by adding the calculated increment of the angular velocity, to the angular velocity calculated automatically by PFC at every time step (Equation 14).

$$\omega_i^{(t)} = \omega_i^{(t)} + \Delta\omega_{rr,i} \tag{15}$$

According to these considerations, the rolling resistance is an eccentricity c_{rr} or sag function u_{rr}. The deeper the block sags, the greater is the rolling resistance $\Delta\omega_{rr}$. In classical mechanics, the rolling resistance is a function of the ratio of the eccentricity c_{rr} to the radius r.

$$\mu_r = \frac{c_{rr}}{r}[-] \cdot \tag{16}$$

This means that spherical blocks of different sizes have the same runout for the same rolling resistance coefficient.

In nature, however, it can be observed that large blocks generally have a longer runout than smaller ones. Therefore, according to the damping model described, the runout is calibrated by the sag u_{rr}.

Figures 10a-10d show model calculations carried out by PFC, using the model of rolling resistance just described. The detached rock mass was modelled as an irregular assembly of particles (Fig. 10a) of two different sizes (r1 = 0.8 m, r2 = 1.6 m). For both particle sizes, the same sag of u_{rr} = 25 cm was employed. Figure 10b shows the position of the runout and figures 10c and 10d show a detailed view of the runout. It therefore became apparent that the larger particles have a longer runout than smaller ones. Fig. 10d shows that within the deposit mass the smaller particles (r = 0.8 m) rest at the bottom and the larger particles (r = 1.6 m) at the top. This model behaviour corresponds closely to observations in nature.

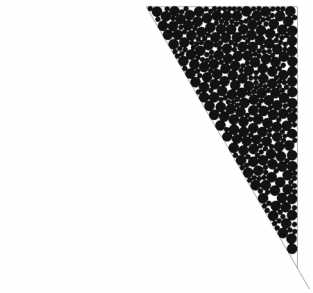

Figure 10a. Detached rock mass

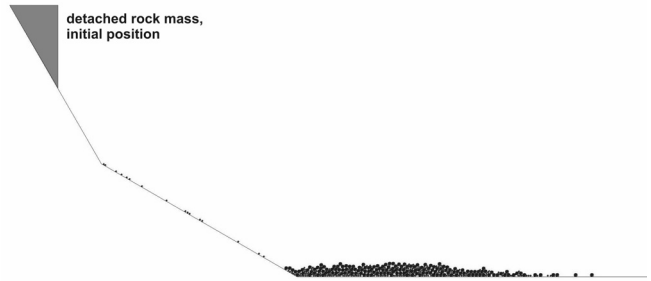

Figure 10b. Final state of the PFC^{2D} calculations

Figure 10c. Deposit

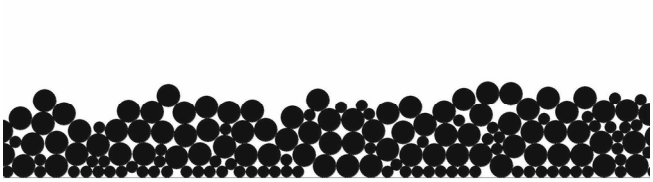

Figure 10d. Deposit, detail view

2.4 *Sliding*

Sliding is calculated by the slip model implemented in PFC without any further adaptation.

3 CONCLUSION

The model described above was used to calculate the runout distances and the risks of the mass movement Lärchberg – Galgenwald (Austria; Fig. 11; Poisel et al. 2007).

With the help of the adapted PFC code it is possible to create a mechanically correct model of rock mass falls. A realistic prognosis of runouts necessitates a calibration of relevant runout model parameters by back calculation of silent witnesses (blocks having fallen down already).

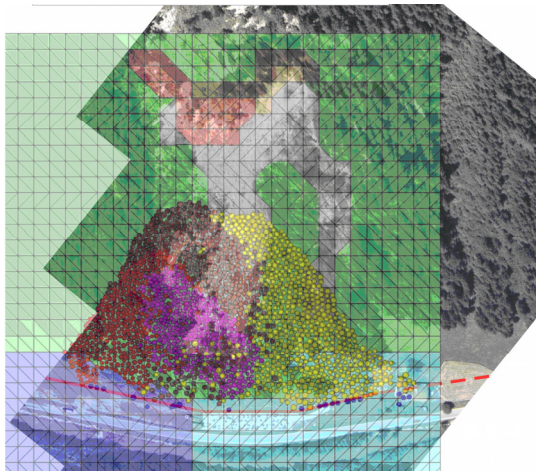

Figure 11. Plan view of final state of runout simulation of a rock mass fall using PFC^{3D}.

REFERENCES

Bozzolo, D. 1987. Ein mathematisches Modell zur Beschreibung der Dynamik von Steinschlag. *Dissertation Nr. 8490 an der ETH Zürich.*

Broilli, L. 1974. Ein Felssturz im Großversuch. *Rock Mechanics,* Suppl. 3, S. 69-78.

Cundall, P.A. 1987. Distinct Element Models of Rock and Soil Structure. In *Analytical and Computational Methods in Engineering Rock Mechanics*, Ch. 4, pp. 129-163, E. T. Brown, Ed. London: Allen & Unwin.

Frühwirt, Th. 2004. Numerische Untersuchungen von Felsmassenstürzen im Bereich der Großhangbewegung Galgenwald bei Murau mittels PFC^{3D}. *Diplomarbeit am Institut für Ingenieurgeologie der Technischen Universität Wien*.

Hoek, E. 1987. Rockfall – A program in basic for the analysis of rockfalls from slopes. Dept. Civil Eng., University of Toronto, Toronto.

Itasca 1999. PFC^{2D} (Particle Flow Code in 2 Dimensions) User's Guide. Itasca Consulting Group, Inc., Minneapolis.

Poisel, R., Angerer, H., Pöllinger, M., Kalcher, T. & Kittl, H. 2007. Risk Management of the Landslide Lärchberg – Galgenwald (Austria). *Proceedings of the 11th Int. Congr. ISRM, Lisbon*.

Poisel, R. & Preh, A. 2004. Rock slope initial failure mechanisms and their mechanical models. *Felsbau* 22: 40-45.

Poisel, R &, Roth, W. 2004. Run Out Models of Rock Slope Failures. *Felsbau* 22: 46-50.

Preh, A. 2004. Modellierung des Verhaltens von Massen-bewegungen bei großen Verschiebungen mit Hilfe des Particle Flow Codes. *PhD Dissertation, Inst. for Eng. Geology*, *Vienna University of Technology*.

Roth, W. 2003. Dreidimensionale numerische Simulation von Felsmassenstürzen mittels der Methode der Distinkten Elemente (PFC). *PhD Dissertation, Inst. for Eng. Geology, Vienna University of Technology*.

Spang, R.M. & Rautenstrauch, R.W. 1988. Empirical and mathematical approaches to rockfall protection and their practical applications. *Proceedings of the 5th International Symposium on Landslides, Lausanne*, Vol. II, pp. 1237-1243.